Author's Accepted Manuscript

www.elsevier.com/locate/csr

Distribution of natural disturbance due to wave and tidal bed currents around the UK

Lucy M. Bricheno, Judith Wolf, John Aldridge

PII: S0278-4343(15)30058-3
DOI: http://dx.doi.org/10.1016/j.csr.2015.09.013
Reference: CSR3282

To appear in: *Continental Shelf Research*

Received date: 16 February 2015
Revised date: 28 August 2015
Accepted date: 10 September 2015

Cite this article as: Lucy M. Bricheno, Judith Wolf and John Aldridge Distribution of natural disturbance due to wave and tidal bed currents around th UK, *Continental Shelf Research,* http://dx.doi.org/10.1016/j.csr.2015.09.013

Abstract

The UK continental shelf experiences large tidal ranges and winter storm events, which can both generate strong near-bed currents. The regular tidal bottom currents from tides plus wind driven 'benthic storms' (dominated by wave-driven oscillatory currents in shallow water) are a major source of disturbance to benthic communities, particularly in shallow waters. We aim to identify and map the relative impact of the tides and storm events on the shallower parts of the North West European continental shelf.

A ten-year simulation of waves, tides and surges on the continental shelf was performed. The shelf model was validated against current meter observations and the Centre for Environmental, Fisheries and Aquaculture Science (CEFAS) network of SmartBuoys. Next, the model performance was assessed against seabed lander data from two sites in the Southern North Sea; one in deep water and another shallow water site at Sea Palling, and a third in Liverpool Bay. Both waves and currents are well simulated at the offshore Southern North Sea site. A large storm event was also well captured, though the model tends to underpredict bottom orbital velocity. Poorer results were achieved at the Sea Palling site, thought to be due to an overly deep model water depth, and missing wave-current interactions. In Liverpool Bay tides were well modelled and good correlations (average R–$squared$=0.89) observed for significant wave height, with acceptable values (average R–$squared$=0.79) for bottom orbital velocity.

Using the full ten-year dataset, return periods can be calculated for extreme waves and currents. Mapping these return periods presents a spatial picture of extreme bed disturbance, highlighting the importance of rare wave disturbances (e.g. with a return period of 1 in 10 years). Annual maximum currents change little in their magnitude and distribution from year to year, with mean speeds around 0.04 ms^{-1}, and maximums exceeding 3 ms^{-1}. Wave conditions however are widely variable throughout the year, depending largely on storm events. Typical significant wave heights (Hs) lie between 0.5 – 2 m, but storm events in shallow water can bring with them large waves of 5 m and above and up to 18 m in North West Approaches / North West Scotland (Sterl and Caires 2005).

The benthic disturbance generated by waves and currents is then estimated by calculating the combined force on an idealised object at the bed. The patterns of this disturbance reflect both regular tidal disturbance and rare wave events. Mean forces are typically 0.05 - 0.1 N, and are seen largely in areas of fast currents ($>$ 1ms^{-1}). The pattern of maximum force however is more dependent on water depth and exposure to long-fetches ($>$ 1000km) suggesting it is dominated by wave events.

Distribution of natural disturbance due to wave and tidal bed currents around the UK

Lucy M Bricheno[a], Judith Wolf[a], John Aldridge[b]

[a]National Oceanography Centre, Joseph Proudman Building, 6 Brownlow Street, Liverpool, L3 5DA, UK
[b] Centre for Environment, Fisheries & Aquaculture Science (CEFAS). Pakefield Rd, Lowestoft, Suffolk, NR33 OHT, UK

Keywords:
bottom disturbance, waves, tidal, ocean model, wave model, UK Continental shelf

1. Introduction

The UK continental shelf experiences large tidal ranges, generating periodic and locally large near-bed currents, as well as winter storm events, which generate strong near-bed currents and also wind waves. These 'benthic storms' are a major source of disturbance for benthic communities. The impact of these disturbances will depend on (i) the sediment type present (ii) bottom stress and (iii) the ability of benthic organisms to cope with displacement or a rapid accretion of sediment (Cooper et al. 2007; Warwick and Uncles 1980; Maurer et al. 1981a,b; Schratzberger et al. 2000; Dernie et al. 2003). Organisms can be threatened by movement of sediment leading to smothering, as well as by the direct impact of hydrodynamic stress in displacing anchored animals and plants. The former effect is examined in a companion paper (Aldridge et al. in press) while this paper focuses on the direct effect of nearbed wave and current velocities.

Many studies have focused on recovery of sites after anthropogenic disturbance, either following dredging for aggregate material, or the disposal of maintenance dredging material e.g. Bolam and Rees (2003), Bolam et al. (2004). Natural disturbances also cause resuspension and restructuring of soft sediments at the seabed (Hall 1994; Levin 1995). If the disturbance is weak, then some fauna can 'dig themselves out' of a burial, generating bioturbation but little change to the overall community. (Cooper et al. 2007). After a major disturbance the benthic community recovers mainly by re-colonisation, then succession (Levin 1995). Cooper et al. (2007) identify faunal types better suited to life in high-energy environments which display characteristics including rapid reproduction, short life span and high mobility and dispersal.

The natural level of bottom disturbance determines which species will inhabit the seabed (Hemer 2006). Herkul (2010) assesses the impacts of physical bed disturbance on sediment properties and benthic communities in the Baltic Sea. Wave exposure significantly affects the biomass and abundance of benthic animals, with recolonisation found to be higher in sheltered sites. Dernie et al. (2003) investigates the response of marine benthic communities within a variety of sediment types to physical disturbance,

Email address: luic@noc.ac.uk (Lucy M Bricheno)

raising the issue that faunal recovery rates will depend on local hydrodynamics, which will be very strongly affected by changing weather conditions.

This work is motivated by the potential impacts of natural disturbances on benthic habitats and communities. We aim to identify the relative impact of tides and storm events at the sea bed of the UK continental shelf by mapping the exposure over a 10-year period, and calculating a representative measure of bed disturbance. The forces generated by waves and tidal currents will be considered separately, before conclusions are drawn about their potential impact at the bed. While the disturbance generated by tides is regular and predictable, wave generated currents can be produced at the bed irregularly in the form of sudden storm events. These short violent episodes can affect areas of the sea-bed which are not commonly disturbed by the regular tidal currents. Wave and tidal near-bed currents depend on water depth in different ways, and wave induced currents (especially those generated by long period waves) regularly penetrate down to the sea bed in coastal areas (Draper 1967).

Before moving to the core issue of bed disturbance, it is important to understand the driving processes of wind-waves and tidal and surge currents. Fortunately the UK continental shelf has been the subject of many studies of tides, waves and coastal change using models and observations. The tides and hydrodynamics of the UK continental shelf has been extensively studied, e.g. Flather (1976), Griffiths (1996), Jones (2002). Most relevant to our work is the study of Holt and James (2001b) who simulated the barotropic tides and the residual currents of the UK continental shelf for a year, at a resolution of 12km. They conclude that their model domain is suitable for a long term study of transport around the UK coast. Early work on storm surge began with Heaps (1977) and modelling methods are reviewed in Bode and Hardy (1997). Storm surge forecasting models are presently run operationally with a predictive range of 36 hours (Williams and Horsburgh 2010). The state and variability of the wave climate has also been well studied e.g. Draper (1980), Draper (1991), Woolf et al. (2002), and wave models are also routinely run operationally (Janssen 2008). Most recently, Brown et al. (2010) performed a wave/tide/surge model hindcast for the Irish Sea. We extend their work by performing a shelf-wide model hindcast, and by making predictions about extreme waves and the impact on bottom stresses.

In this study wave and tidal bed-shear stresses are calculated from a 10-year model hindcast of tides, surge and waves on the northwest European shelf. Modelling and observation methods are presented in sections 2a and 2b respectively. Shelf-wide validation of wave and tidal conditions is presented in section 3a. In section 3b, the modelled bottom velocities and pressures are validated against in-situ observations. In these data sets wave and current data were observed simultaneously, giving a unique opportunity to investigate combined wave and bed disturbances. By using the full 10-year hindcast, estimates of the frequency of bottom disturbance by waves and currents are presented in section 4. In section 5 a measure of force on an idealised object, representing a benthic organism, is introduced. This can be used to compare the relative disturbance at the bed across the whole continental shelf. This combined bottom force associated with waves, surges and tides is then mapped, to give a spatial picture of the seabed climate and implications for sediment transport around the coastal seas of Britain. The results are discussed in section 6 and summarised in section 7.

2. Methods

a. *Hydrodynamic and wave model*

In this study we use the Proudman Oceanographic Laboratory Coastal Ocean Modelling System (POLCOMS) (Holt and James 2001a) to simulate hydrodynamics, and waves the 3rd-generation spectral model WAM (Komen et al. 1994), adapted for shallow water applications (Monbaliu et al. 2000) is used for waves. The shallow water adaptations include depth-induced breaking (Battjes and Janssen 1978) and the introduction of a wave–current bottom friction (e.g. Madsen (1994)). The models are run in an uncoupled mode.

A coarse resolution, deep water wave model run was performed to generate the wave boundary forcing for the continental shelf. The outer model covers the North East Atlantic (NEA) domain, extending from 40 to 65° North and from -25 to 15° East, with a 1° resolution. The NEA Model is forced with 6 hourly winds, at a 1° resolution, provided from the ERA-40 model run by the European Centre for Medium-Range Weather Forecasts (ECMWF) (Uppala et al. 2005). No wave boundary forcing is applied to the open boundary of this model.

Tides, storm surges and waves on the European Continental shelf have been simulated for the ten year period from 1999 to 2008 inclusive. The continental shelf model extends from 48 to 64° North and from -12 to 13° East, with a spatial resolution of $\frac{1}{9} \times \frac{1}{6}^\circ$ i.e. $\approx$ 12km. Figure 1 shows the extent of the model domain, and the sites used for model validation. The tide was simulated using the 15 tidal constituents (Q_1, O_1, P_1, S_1, K_1, $2N_2$, μ_2, N_2, ν_2, M_2, L_2, T_2, S_2, K_2 and M_4). The POLCOMS model was forced with spectral tides at the open boundaries, and 12km hourly wind and pressure data from the UK Met Office mesoscale atmospheric model (Davies et al. 2005) at the surface. A minimum water depth of 10m was applied to avoid treating wetting and drying conditions at the coast. Effects of temperature and salinity have not been included, as a constant density was used throughout the simulations and density effects are negligible for the present application.

POLCOMS uses a constant roughness length of 0.003 m, and WAM calculates bottom friction using the Madsen method. The POLCOMS model generates hourly output maps of 3d currents, water levels, and bed-stresses. From the wave model maps of integrated wave parameters and bed shear stress statistics were extracted hourly, together with the wave-orbital speed and direction, shear velocity and the wave friction factor.

b. *Wave and current observations*

Data sets which observe wave and current data simultaneously are available at three sites: (a) The Southern North Sea (SNS) 53°10.123'N, 02°48.416'E in 31m water depth (b) Liverpool Bay (LB) 53°32.07N', 03° 21.35'W, in about 20-25m water depth (Howarth et al. 2006; Wolf et al. 2011) and (c) Sea Palling (SP) 52°48.09'N 1°35.38'E in 5.4m water depth (Pan et al. 2010; Wolf et al. 2008, 2010).

At the Southern North Sea site, CEFAS collected a month long dataset covering parts of January and February 2000. The Minipod instrument recorded current, wave and suspended sediment data at around 1m above bottom. An instrument description

Variable	Sensor	Frequency
Horizontal currents	Marsh McBurney current meter	5 Hz
Suspended sediment at two elevations	Optical backscatter sensor	1 Hz
Suspended particle size information	Acoustic backscatter sensor	2.5 Hz
Tidal elevation and waves	DigiQuartz pressure sensor	5 Hz
Currents and backscatter in water column	Upward-looking ADCP	1 Hz

Table 1: Instrument specifications at the CEFAS Southern North Sea site.

Variable	Sensor	Frequency
Horizontal currents	600 kHz RDI ADCP	10 minutes
3d currents	SonTek ADV-ocean-Hydra	10 minutes
Waves	600 kHz RDI ADCP	100 pings every 10 minutes

Table 2: Instrument specifications at the ISO Liverpool Bay & Sea Palling sites.

can be found in table 1. At the Sea Palling Site the same instrument package is used as that in Liverpool Bay (specifications in table 2), with an ADV current meter and ADCP measuring waves, currents, and water depth.

The observational data have been processed to extract values for significant wave height (Hs), assuming linear wave theory. For a monochromatic wave the bottom orbital velocity is usually defined as the amplitude of the oscillatory bottom velocity, U_b. This is related to the surface elevation (ζ) time series, by taking account of the wave attenuation with water depth:

$$\zeta = a\cos(kx - \omega t) \tag{1}$$

Equation (1) gives the surface displacement for an individual monochromatic wave, of amplitude a, angular frequency ω ($\omega = 2\pi f$, where f is the wave frequency in Hz) and wave-number k ($k = 2\pi/\lambda$, where λ is the wavelength). (NB this equation can also be applied to a tidal wave, it simply gives the definition of a progressive sine wave). Then we have

$$U_b = \frac{\omega\zeta}{\sinh(kh)} \tag{2}$$

In order to get the bottom velocity spectrum, $S_u(\omega)$ from the surface elevation spectrum, $S(\omega)$, the approach of Wiberg and Sherwood (2008) is followed:

$$S_u(\omega) = \frac{\omega^2}{\sinh^2(kh)} S(\omega). \tag{3}$$

The root mean square of the bottom orbital velocity is then equal to the representative bottom orbital velocity Madsen (1994), U_{br}, given by

$$U_{br} = \sqrt{2\int S_u(\omega) d\omega}. \tag{4}$$

The surface wave spectrum can be obtained from bottom velocities by inversion of this process. However, the values for observed surface wave height may be under– or over–predicted by this analysis in deep water. For example, at the SNS site after correcting for mean atmospheric pressure (1012 mb) the maximum water depth was found to be 31 m, which is usually regarded as too deep for observing higher frequency waves at the seabed due to depth attenuation. The analysis of bottom pressure and current data to obtain surface waves is critically dependent on the high-frequency cut off (Wolf 1997). The bottom wave-induced velocity here has been calculated directly from the high-frequency 'burst' current meter data (by removing the mean) and therefore is a direct measurement of the wave-orbital current near the bed with no assumptions made in its calculation. We do expect some discrepancy between this measured value and the modelled result, as the observations will include effects of tidal turbulence and interactions. The wave model WAM was run uncoupled from POLCOMS, so no tidal modulations are expected in this 'wave-only' version of the U_{br}.

3. Validation

The POLCOMS-WAM model has been validated for the UK Continental shelf and the Irish Sea in previous studies e.g. Brown et al. (2010) ran the coupled model to investigate model surge elevations. A percentage model bias is calculated, defined by Maréchal (2004) as

$$Pbias = 100\frac{\Sigma_{n=1}^{N}(M_n - D_n)}{\Sigma_{n=1}^{n} Dn} \tag{5}$$

where M_n is the model prediction and D_n represents the data for a number of observations N. Brown et al. (2010) also calculate a cost function CF which represents the goodness of fit, defined as

$$CF = \sqrt{\frac{1}{N\sigma_D^2}\sum_{n=1}^{N}(Mn - Dn)^2} \tag{6}$$

where σ_D represents the standard deviation of the data. $Pbias$ provides a measure of whether the model is systematically over- or under- predicting the measured data. For the Irish Sea, they find a cost function < 0.6, with $Pbias$ generally $< 30\%$ and often $< 10\%$ for POLCOMS. For WAM, a CF < 0.7 is found for significant wave height and $Pbias < 38\%$. Less than 10% is thought to be excellent, and $20 - 40\%$ is good (Allen et al. 2007). Brown (2010) also assessed a POLCOMS-WAM model hindcast performance at the Liverpool Bay buoy in January 2007, finding a $PBias$ of -0.64 with an $rmse$ error of 0.24m in surge elevation.

Here, the model performance is measured by considering significant wave height, and current speed and direction at a representative set of stations a in the North , Irish and Celtic seas (Figure 1). For the wave model a root mean-square error ($rmse$) and correlation (R–$squared$) were calculated additionally to the $Pbias$. The model validation first considers shelf-wide performance of the surface wave and depth-mean current model, before focusing on the bottom disturbance generated by waves and currents. At

Site	Lat	Lon	Depth	$Pbias$, %	$R\text{–}squared$	$rmse$, m
Poole Bay	50°37'.100N	1°43'.17W	28m	-7.84	0.85	0.06
Hastings	50°44'.76N	0°45'.20E	43m	-28.20	0.89	0.03
Dungeness	50°54'.18N	0°58'.44E	31m	-22.51	0.85	0.04
Tyne Tees	54°55'.12N	0°44'.94W	65m	-23.53	0.78	0.13
Sizewell	52°12'.48N	1°41'.06E	18m	-7.62	0.88	0.04
Dowsing	53°31'.84N	1°03'.30E	22m	-16.83	0.85	0.05
Moray Firth	57°57'.99N	3°20'.01W	54m	-25.16	0.56	0.22
Firth of Forth	56°11'.28N	2°30'.23W	65m	-20.46	0.59	0.06
Liverpool Bay	53°31'.100N	3°21'.18W	24m	-31.44	0.69	0.07
Scarweather	51°25'.100N	3°55'.100W	35m	-13.06	0.88	0.05
Average				-19.67	0.78	0.077

Table 3: Pbias, $R\text{–}squared$ error, $rmse$ for modelled Hs at 10 sites on the UK continental shelf

the sites where bottom observations are available, wave period, bottom orbital velocity and water-levels can also be examined.

a. *Shelf-wide validation*

The UK wave buoy network, WaveNet (www.cefas.co.uk/wavenet), was used as a source of validation data for the WAM model. In order to get a good spatial coverage of observations on the continental shelf, December 2008 was chosen as a validation month. During this period there are 10 WaveNet buoys recording data. The positions of the buoys used are plotted as blue crosses in Figure 1

Table 3 presents statistics relating to the performance of the wave model for these 10 sites across the UK continental shelf. The wave model is generally seen to under-predict Hs, particularly at low wave heights (also demonstrated in detailed results in section b) as indicated by negative values of $Pbias$. The $R\text{–}squared$ correlations give an indication of how well temporal variability is captured by the wave model. The average correlation is 0.78, with the poorest agreement seen in Moray Firth and the Firth of Forth. The variability is particularly well captured in Hastings, Sizewell and at the Scarweather buoy. Overall the $rmse$ are acceptable, with errors between 3cm at Hastings and 22cm in the Moray Firth. The errors are largest at the more enclosed locations of Moray Firth and the Firth of Forth: here the errors are at least double those seen elsewhere. A good agreement is seen at all other sites, particularly the more exposed coastal sites, e.g. Sizewell and Hastings.

In order to validate the tidal model, M2 depth mean U and V current amplitudes and phases were compared with a set of moored current meters at 15 points around the shelf as used by Davies and Kwong (2000). The locations of observations are show in Figure 1, and the closest model point is extracted for comparison. The current meter data were selected from the middle of the water column as this is likely to be most representative of the depth mean value. The results are plotted in Figure 2 and suggest no clear bias between over and under-prediction of either amplitudes or phase. However some model values deviate considerably from the observed val-

Variable	$Pbias$, %	$R–squared$	$rmse$
U amplitude	-10.27	0.95	0.064 ms $^{-1}$
V amplitude	20.14	0.88	0.074 ms $^{-1}$
U phase	-3.56	0.61	35°
V phase	29.21	0.76	36°

Table 4: Model performance for M2 tidal phase and amplitude.

Table 5: $R–squared$ correlation and $rmse$ for U_{br} and Hs in Liverpool Bay

Deployment	Start	End	U_{br} $R–squared$	U_{br} $rmse$	Hs $R–squared$	$Hsrmse$
40	01/11/2006	19/12/2006	0.779	0.0014 ms $^{-1}$	0.890	0.129 m
41	13/12/2006	15/02/2007	0.667	0.0032 ms $^{-1}$	0.861	0.272 m
49	21/11/2007	11/01/2008	0.828	0.0009 ms $^{-1}$	0.873	0.143 m
50	11/01/2008	14/03/2008	0.887	0.0009 ms $^{-1}$	0.923	0.106 m

ues. More information about the observations can be found on the BODC website. `https://www.bodc.ac.uk/data/`.

Table 4 shows some statistical analysis of the tidal model performance, including root mean squared error ($rmse$) and coefficient of determination ($R–squared$ which varies between zero and one). The model performs well for current amplitudes, with high correlations. The phases is less well resolved, with typical errors of the order 35 °. The model performs well in the Irish Sea, and Southern North Sea, but some errors in phase are observed close to the location of tidal amphidromes. Modelled phases do not show any consistent bias, but tidal ellipses (not shown) demonstrate that the model is able to distinguish between rotating and rectilinear tides.

b. *Near-bed high frequency current and wave data*

i. Liverpool Bay High-frequency burst data were collected at the Liverpool Bay site for several deployments between 2003 and the present day. Four deployments were chosen for model validation, during periods of storms and high wave activity (Table 5). The correlations and $rmse$ are presented in Table 5, showing that the model captures significant wave height very well with a mean $R–squared$ of 0.887. U_{br} is less well modelled with a mean correlation of $R–squared$ =0.790. However, the absolute error is very small (of the order 0.001 ms $^{-1}$). The mean error in Hs is 0.16 m.

Figure 3 shows a comparison between modelled and observed tidal current speed and bottom orbital velocity for deployment 49 (detailed in Table 5). The variability of both U_{br} and tidal currents are well captured, though some discrepancy is seen in Hs (not shown) at low wave heights during days 1-14, where the model produces larger waves than observed.

ii. Southern North Sea Figure 4 shows time series of water levels and bottom orbital velocities at the Southern North Sea site. During the period of observations three bottom disturbance events occurred: around days 23, 30, and 40. The maximum non-tidal residual water level was observed during a neap tide on day 30, corresponding to a surge elevation > 1.5m. Two large wave events were observed with Hs (not shown) reaching 3.5 m on January 30th 2000, and 4.24 m on February 9th 2000. Some tidal modulation in the bottom orbital wave velocity (U_{br}) is observed, with quarter-diurnal oscillations, however as the models were run in uncoupled mode, this is not simulated by the wave model. The depth integrated current speed (not shown) is not obviously affected by the passing storms.

During calm periods Hs (not shown) tends to be over–predicted at this deep water site, as it is derived from bottom velocities where high frequency waves are attenuated leading to this overestimation (see section 2b). The water levels show both the phase and amplitude of both tide and surge are adequately modelled by POLCOMS at this site. As the datum is not know, the modelled water levels are plotted with an offset of the mean of the observed water level during the period of observations. The signature of the storm surge is clearly visible on day 30, and also reflected in the U_{br}. The model tends to under–predict bottom orbital velocity, it is likely that, as a global wave model is not being used, very long swells will be underpredicted (as seen in e.g. Leake et al. (2007)). The wave period Tp is also found to be too short in the model, confirming that the long waves causing large disturbance at the bed are missing.

iii. Sea Palling The third site where high frequency data were recorded is in the shallow coastal zone off Sea Palling. More background about the observations made at this site can be found in Pan et al. (2010) and Wolf et al. (2008). Here a progressive tide dominates, with current speeds of up to 0.60 ms^{-1}. The model is able to simulate the tidal currents adequately, capturing the tidally driven current direction well but underpredicting both speed and tidal amplitude. Significant wave height (Figure 5) and peak wave period (not shown) are well captured during large wave events (the storm on day 305), but the model over–estimates both variables during calm periods.

In the model, the closest grid point was chosen for comparison against observations. The modelled water depth at Sea Palling is 15 m, and the POLCOMS model is restricted to using a minimum depth of 10 m, while the true depth observed is just 5.4 m. As the model resolution is quite coarse (12 km), shallow water close to the coast is particularly difficult to model. Hence there are large difference in water depth between the model and observations here.

Figure 5 shows that the model is unable to capture the wave-tide interactions observed in shallow water, and a coupled model is required here. The tidal modulation of the wave height observed is not captured by the model, as the modelled water-depth is held constant in the spectral wave model. Also, in the observed data it is seen that the regular tidal reversals (shown by the current speed panel in Figure 5) disappear in the observations, during the peak of the storm event on day 304-306. However, the reversals continue in the uncoupled POLCOMS model, which may be because the modelled surge is not large enough. The modelled water depth is too large here, preventing the Kelvin wave from building; with this under-predicted surge, the modelled tidal currents are able to reverse.

4. Climatology and extreme events

Having sampled the data set throughout the modelled period and gained some confidence in the results we now use the full simulation to produce a 10 year climatology. As well as extracting an overall climatology representing mean, maximum and minimum values, we use statistical methods to extrapolate outside our data set and make predictions about extreme events. This section examines in more detail the wave climate on the continental shelf, and the statistics of extreme events.

From the modelled 10 year time series we can extract some typical conditions. Plots of average significant wave height (metres) and peak period (seconds) are shown in Figure 6. Offshore to the West and North of the UK, large long period waves are seen with average Hs in excess of 2 m and average periods of 8–9 s. These represent long-fetch waves generated in the open ocean. The waves are shorter period and lower towards the mouth of the Baltic, the English Channel, the Southern North Sea, and the interior of the Irish Sea. Here, the mean wave heights are around 0.5 m with periods of 5 s and below.

Turning to currents, the majority of the shelf experiences low speeds of the order 0.04 ms^{-1} on average. The largest modelled mean currents are seen along the shelf edge and into the Skaggerak (57.77N, 11.20E) with typical values of 0.20 ms $^{-1}$. The maximum currents simulated by the model (not shown) also vary very little year-on-year, as they tend to be tidally generated. Figure 7 shows the typical distribution of the maximum current speeds. The largest speeds are associated with tidal currents through straits and around headlands, for example in the Pentland Firth, English Channel and around Anglesey. The annual maximum currents reach 2–3 ms $^{-1}$

To examine interannual variability, a mean annual maximum, and standard deviation of current speed and significant wave height were calculated. These values are then spatially averaged across the whole model domain. The modelled currents have a mean annual maximum of 0.38 ms^{-1}, and a standard deviation of 0.40 ms^{-1}. The mean annual maximum has the same overall distribution and maxima as that shown for the example year (2006) in Figure 7. Hs has a mean annual maximum of 7.49 m, and a standard deviation of 0.65 m. This large mean annual maximum demonstrates the large interannual variability associated with the same field. The standard deviation of Hs has a similar spatial distribution at the mean Hs, with values typically around half the magnitude of the annual mean waveheight. The standard deviation of current speed is $\approx 10\%$ of the mean value, while the standard deviation for Hs is $\approx 50\%$ of the mean value.

In order to extrapolate beyond the 10 year data set, and make estimates of the climate of waves and currents on the continental shelf, an extreme value method is used. Extreme value methods are statistical techniques used to describe the tail of the distribution of known data. They are particularly suited to distributions with long tails (and so well suited to the distribution of wave heights in this region), in order to make predictions about rare events. The approach used is detailed in Coles and Tawn (1991), and for this study we use a Weibull distribution (Weibull 1951). The probability density function of a Weibull random variable X is fitted using two positive parameters: the shape parameter, k and the scale parameter λ. The probability density function is defined as:

$$f(X;\lambda,k) = \begin{cases} \frac{k}{\lambda}\left(\frac{x}{\lambda}\right)^{k-1} e^{-(x/\lambda)^k} & x \geq 0, \\ 0 & x < 0, \end{cases} \tag{7}$$

By fitting a Weibull distribution to, for example, modelled significant wave height we can make a prediction of the maximum Hs that can be expected at a particular point within a given length of time or ‘return period’. Figure 8 shows the maximum significant wave heights reached for return periods of 1 and 50 years.

We can compare our findings with Wolf (2008) who use wave data from 2002–2006, finding the 1 in 50 year wave height in Liverpool Bay is about 5.5 m. At the closest model grid point to the buoy observations (located at 3°32’.07N, 003°21’.44W) we predict a 1 in 50 year wave height of 6.6 m, which also compares well with the findings of Wolf et al. (2011). Errors in the Weibull fit can be read as confidence intervals to our predictions. To make sure unique events are considered, they must be separated by a minimum of 6 hours. When using the 10 largest values of wave height for each year (i.e. 100 records) we find a 0.5% error in the shape parameter and an error of 4.5% in the scale parameter.

The extreme value approach can also be applied to the currents, but little difference is seen between the 1 and 50 year return period (Figure 9), as the currents are dominated by tides, and shallow water wave induced currents are not included in this simulation. Tidally dominated areas, such as the English Channel, Anglesey and the East coast see little change between return periods. However where the tides are weak, and the wind driven component dominates some differences are observed, for example around the West coast of Scotland

5. Force on seabed object

In order to translate our modelled wave and current information into a consolidated measure across the shelf, an idealised ’organism’ is used. This should not be thought of as a real animal but rather a way of standardising the forces experienced by an object on the seabed. A 1 cm diameter, 10 cm high cylinder was chosen to represent a benthic organism. The force on a cylinder was modelled using the Morison equation, as described for example in Journèe and Massie (2001). The total force consists of drag and inertia components dependent on the speed and acceleration of the flow respectively. The instantaneous force (per unit cylinder height) is given by

$$F_1(t) = \rho(a_M D^2 \dot{\boldsymbol{u}} + a_D D \boldsymbol{u}|\boldsymbol{u}|) \tag{8}$$

where the local instantaneous velocity at height z is $\boldsymbol{u} = \boldsymbol{u}(t, z)$, the dot represents a time derivative, ρ is water density, D is the cylinder diameter, and $a_M = (\pi/4)C_M$ and $a_D = \frac{1}{2}C_{DW}$ are non-dimensional drag coefficients. Drag and added mass coefficients were taken as $C_M = 1.5$ and $C_{DW} = 1.2$ (Journèe and Massie 2001). The Morison equation is itself an empirical approximation.

Further approximations are made to obtain an estimate of the maximum force over a wave period that is based on the modelled waves and currents. The velocity in 8 is approximated by an average over the cylinder height. Then the maximum of Equation

8 over a wave period is sought when the velocity is a sum of current and wave components $\bar{\boldsymbol{u}} = \boldsymbol{u}_c + \boldsymbol{a}_w \sin\omega t$,where ω is the mean wave frequency (derived from the zero up-crossing period given by the wave model) and $\boldsymbol{u}_c$ and $\boldsymbol{a}_w$ are respectively the current and wave velocities averaged over the cylinder height h_{cy} as described below. The calculation is complicated by the non-linear quadratic drag term which we linearise by fixing $\bar{\boldsymbol{u}}$ at its maximum value given by $M = \max\{|\boldsymbol{u}_c + \boldsymbol{a}_w|, |\boldsymbol{u}_c - \boldsymbol{a}_w|\}$

Substituting into Equation 8 and treating the mean current velocity $\boldsymbol{u}_c$ as constant over a wave period, an approximation for the maximum value of total force on the cylinder (in Newtons) over a wave period is

$$F^* \approx \rho\ D\ h_c\ max\{|a_D M \boldsymbol{u}_c + r\boldsymbol{a}_w|, |a_D M \boldsymbol{u}_c - r\boldsymbol{a}_w|\} \tag{9}$$

where h_c is the cylinder height and $r = \sqrt{(a_M \omega D)^2 + (a_D M)^2)}$. It remains to approximate the mean value of current and wave velocity over the cylinder in terms of the depth mean current $\boldsymbol{U}_c$ and wave orbital amplitude $\boldsymbol{a}_w$ provided by the hydrodynamic and wave model calculations.

A logarithmic current profile is assumed

$$\boldsymbol{v}(z) = k\ \boldsymbol{U}_c\ \ln(z/z_o) \tag{10}$$

derived by assuming bed stress is given by a quadratic law $\tau = \rho C_D |\boldsymbol{U}_c|^2$, where U_c is the depth mean current, $k = \sqrt{C_D}/\kappa$, with von Karman constant κ = 0.4 and where $C_D = [\kappa/(\ln(h/z_0) - 1)]^2$ with $z_0 = k_s/30$, where k_s is the bed roughness. For non-rippled beds k_s can be related to the median seabed grain diameter D_{50} by $k_s = 2,5D_{50}$. The situation where the bed is covered with small scale rippled bedforms is discussed below. For simplicity no account was taken of wave current interaction on the logarithmic profile in Equation 10. The cylinder will lie well within the current benthic boundary layer for any relevant value of the cylinder height. Averaging Equation 10 over the cylinder height h_c gives u_c in terms of the depth average velocity as

$$\boldsymbol{u}_c = k[h_c \ln(h_c/z_0)/(h_c - z_0) - 1.0]\boldsymbol{U}_c \tag{11}$$

The wave boundary layer is generally thin, with typical thickness $\delta_w <$ 1–2 cm (Sana and Tanaka 2007). Thus the cylinder is likely to be partly within and partly outside the wave boundary layer. For calculating δ_w as a function of wave and bed roughness parameters the formulae of Sana and Tanaka (2007) was used. Above δ_w, the wave velocity is assumed to be given by the free-stream amplitude $\boldsymbol{U}_w$ taken in the direction of the mean wave propagation θ with amplitude $|\boldsymbol{U}_w| = \sqrt{2}u_{rms}$ where u_{rms} is the root mean square (rms) value of the wave spectrum. Thus $\boldsymbol{U}_w$ is the amplitude of the monochromatic wave with the same energy as the wave spectrum. Quantities u_{rms} and θ are output by the wave model. For simplicity the velocity profile below δw is assumed to decrease linearly from $|\boldsymbol{U}_w|$ to zero at the bed. Then, averaging over the cylinder height and assuming $\delta w < h_c$ yields $\boldsymbol{a}_w = (1 - \frac{1}{2}\delta_*)\boldsymbol{U}_w$ where $\delta_* = \delta_w/h_{cy}$.

Calculation of the bed roughness was based on bed type (% mud, sand gravel) and median grain diameter taken from the British Geological survey and the North Sea Benthos survey. Median grain size can vary from $<60\mu m$ for muddy regions and greater than 1 cm in gravel regions (Figure 10). Because grain diameter was only measured for the sand fraction, for gravel beds the diameter was estimated based on a correlation between median gravel size and the sand/gravel ratio from a sample of locations as described in Aldridge et al. (in press). For sand beds it may be appropriate to relate the bed roughness to the sand ripples. In this case the z_0 was related to ripple height η by Soulsby (1995);

$$z_0 = z_{0\,\mathrm{grain}} + \eta/7 \tag{12}$$

The bed ripple height was taken as 2 cm which is appropriate for current ripples or small wave ripples. It should be noted that spatial variations in bed roughness were applied during post-processing of the model outputs to obtain the force, the hydrodynamic and wave model runs used a spatially constant bed roughness value.

Simulated wave and current conditions for the year 2000 were used to obtain the statistics of the cylinder force. The annual mean and maximum wave-current force is plotted in Figure 11 (top row) for the non-rippled sand case and Figure 11 (bottom row) assuming a rippled bed where sand is present. Mean force is related to the distribution of tidal current speeds whilst the peaks are related to wave energy with highest values occurring in shallow water (e.g. the Dogger bank in the North Sea) and/or on west facing coasts where wave fetch is highest. The effect of assuming rippled sand beds is quite striking, leading to significant (up to 50%) reductions in the predicted force on sandy substrates due to higher bed roughness decreasing the near bed region velocities for both currents and waves. Over the shelf as a whole this leads to a reduction in the spatial variation of both the mean and maximum force.

The mean force experienced can be as large as 0.3 N, with the maximum combined force reaching 3–4 N in places. The peak forces are observed in areas of fast currents, such as the Dover Straits, but also on South West facing coasts where wave exposure is greater.

6. Discussion

The model is well validated offshore, though some disagreements have been noted close to the coast and in very shallow water. The model is limited by not considering wetting and drying, or wave-current interactions. Nevertheless, extreme events during storms seem to be well captured in the models, giving us confidence in the derived climatologies. The use of a Weibull extreme value distribution allows us to extrapolate beyond our 10-year data set, and predict extreme waves and currents for longer return periods e.g. 50 years. Little change is seen between the magnitude of 1 and 50 year return values for current speeds where tidal currents dominate, however differences are larger in areas where wind driven residual currents are dominant. The wave height return levels are more variable, with values of Hs up to 12m observed to the North of Scotland. It is these large (and often long-period) waves which will penetrate deep into the water column, impacting the bed.

Neill et al. (2010) present modelled tide, wave, and combined shear stresses for the same region. They compare the present day UK shelf seas with a palaeobathymetry, showing the importance of relative sea level on bottom stresses. They conclude that the residual and relative distribution of bed shear stress were generally insensitive to interannual variability. We argue that interannual variability becomes more important when we consider extreme events which though not contributing significantly to the mean stress, have major impacts at the seabed and potentially on benthos.

Consideration of the force on a seabed object suggest that the mean force is associated with distribution of tidal currents while the extreme forces are associated with storm events with the latter particularly prominent on westward facing coasts or shallow regions like the Dogger Bank . The results over sand were found to be quite sensitive to whether ripples are assumed to be present due to the assumptions about how near bed wave and current velocities vary with bed roughness. If realistic this potentially makes the force on a nearbed organism in a region with lower depth mean current but a smooth bed (e.g. mud) comparable with that in a region with higher depth-mean current where the bed is rippled. If so relating potential biological effects to depth mean current (or the bed stress calculated from it) may be misleading. However, it might also be argued that the extra roughness provided by the ripples will increase the near-bed turbulence and this will compensate for the slowing of the mean velocity. Further work would be required looking in detail on the forces on nearbed objects with and without bed ripples to decide this. Clearly the division into fixed height rippled and non-rippled beds used here is a rough indication of effect only, bedform height will vary dynamically with flow conditions for example and under sheet flow conditions (Myrhaug and Holmedal 2007) bedforms will disappear entirely. Nevertheless the calculations here may have highlighted an effect of small scale bedforms in decreasing near-bed velocities that may be of biological relevance.

The work here addresses the possible biological implications of the spatial variation in wave and current intensity on the European shelf by considering the force on a hypothetical object (cylinder) at the seabed. This is an appropriate way of assessing the magnitude of the physical drag forces on organisms living at the sediment surface and for assessing the relative ‘harshness’ of a given benthic environment. A complementary approach is to consider the disturbance to the seabed itself with the assumption that seabed disturbance leads to disturbance of organisms both in and on the bed. This requires a much more detailed consideration of the bed substrate and the conditions and mode of disturbance it will undergo under different wave and current conditions. This is considered in a companion paper Aldridge et al. (in press) which uses the same wave and current forcing as in this study but makes use of sea bed characteristics to investigate the number of days per year during which the sea-bed is naturally disturbed.

7. Summary

A ten year hindcast of waves, surges and tides was run (without wave-tide-surge coupling) in order to investigate exposure to wave and current generated disturbances at the bed. The model was first validated for wave height and current speed and direction over the UK Continental shelf. The tidal model performed well in general, with some discrepancies seen close to amphidromic points. The wave model also gave good results, particularly during extreme events. Low wave heights tend to be underpredicted, leading to poorer results in sheltered sites.

Next, high frequency seabed lander observations were used to focus on model performance at the bed. Water levels and current speeds were well captured at all sites, and large Hs and Tp were also well captured during storm events. The model performance was worst in very shallow water, due to the minimum water depth assumption and models being run uncoupled and therefore unable to capture tidal modulation of the wave field or wave-current interaction.

A modelled climatology showed certain areas to be regularly exposed to fast tidal currents, which varied little year on year. The wave climatology was more spatially varied, with South-West exposed coasts, and shallow water areas identified as at risk from large waves.

By fitting an extreme value distribution to the wave data, an extrapolation can be made about possible damage by extreme waves. In contrast, the extreme value fit for currents showed little change when deriving a 1-year return period and a 50-year return period.

Finally the force on an idealised benthic object was calculated: combining the effects of waves and currents simultaneously. Mapping these forces gives a spatial picture of the total bed disturbance, which is comparable across the whole continental shelf. This work has allowed us to gauge the importance of waves and currents to organisms at the bed. These maps could be of use for identifying suitable habitats for benthic organisms, as well as determining the chances of exposure to dangerous benthic storms.

a. *Acknowledgements*

This work is funded by the Aggregate Levy Sustainability Fund (ALSF) under contract MEPF 09-P114 and NERC National Capability funding. The views expressed are those of the authors and do not reflect the policies of the funding department.

J. N. Aldridge, E. R. Parker, L. M. Bricheno, S. L. Green, and J. van der Molen. Assessment of the physical disturbance of the northern European Continental shelf seabed by waves and currents . *Cont. Shelf Res.*, pages –, in press.

J. I. Allen, J. T. Holt, J. Blackford, and R. Proctor. ”error quantification of a high-resolution coupled hydrodynamic-ecosystem coastal-ocean model: Part 2. chlorophyll-a, nutrients and spm”. *J. Marine Sys.*, 68(3):381–404, 2007.

J. A. Battjes and J. P. F. M. Janssen. Energy loss and set-up due to breaking of random waves. *Proc. 16th Int. Conf. Coastal Eng*, pages 569–587, 1978.

L. Bode and T. Hardy. Progress and recent developments in storm surge modeling. *J. Hydraulic Eng*, pages 315–331, 1997.

S. G. Bolam and H. Rees. Minimising the impacts of maintenance dredged material disposal in the coastal environment: a habitat approach. *Environ. Manage*, 32:171–188, 2003.

S. G. Bolam, P. Whomersley, and M. Schratzberger. Macrofaunal recolonization on intertidal mudflats: effect of sediment organic and sand content. *J. of Experimental Marine Biology and Ecology*, 306:157–180, 2004.

J. M. Brown. A case study of combined wave and water levels under storm conditions using WAM and SWAN in a shallow water application. *Ocean Modelling*, 35:215–229, 2010.

J. M. Brown, A. Souza, and J. Wolf. An 11-year validation of wave-surge modelling in the Irish Sea, using a nested POLCOMS-WAM modelling system. *Ocean Modelling*, 33:118–128, 2010.

S. G. Coles and J. A. Tawn. Modelling extreme multivariate events. *Journal of the Royal Statistical Society. Series B (Methodological)*, pages 377–392, 1991.

K. Cooper, S. Boyd, J. Aldridge, and H. Rees. Cumulative impacts of aggregate extraction on seabed macro-invertebrate communities in an area off the east coast of the United Kingdom. *J. Sea. Res.*, 57:288–302, 2007.

A. M. Davies and S. C. M. Kwong. Tidal energy fluxes and dissipation on the European continental shelf. *J. Geophys. Res. C*, 9:21969–21969, 2000.

T Davies, MJP Cullen, AJ Malcolm, MH Mawson, A Staniforth, AA White, and N Wood. A new dynamical core for the Met Office's global and regional modelling of the atmosphere. *Quarterly J. of the Royal Met. S.*, 131(608):1759–1782, 2005.

K. M. Dernie, M. J. Kaiser, and R. M. Warwick. Recovery rates of benthic cimmunities following physical disturbance. *J. Animal Ecology*, 72:1043–1056, 2003.

L. Draper. Wave activity at the sea bed around Northwestern Europe. *Marine Geology.*, 5:133–140, 1967.

L. Draper. The north-west European shelf seas: The sea bed and the sea in motion ii. physical and chemical oceanography, and physical resources. *Elsevier Oceanography Series*, 24:353–368, 1980.

L. Draper. Wave climate atlas of the British Isles. *Offshore Technology Report*, page 11, 1991.

R. A. Flather. A tidal model of the North-West European continental shelf. *Mem. Soc. Roy. Sci. Liege, 6th Ser.*, pages 141–164, 1976.

C. R. Griffiths. *Extreme residual current speeds upon the UK Continental Shelf*. Health and Safety Executive Books, 1996.

S. F. Hall. Physical dsturbance and marine benthic communities: life in unconsolidated sediment. *Oceanography and Marine Biology: an Annual Review*, 32:179–239, 1994.

N. S. Heaps. Development of storm-surge models at Bidston. *POL Internal Document*, 53:64, 1977.

M. A. Hemer. The magnitude and frequency of combined flow bed shear stress as a measure of exposure on the Australian continental shelf. *Cont. Shelf Res.*, 26: 1258–1280, 2006.

K. Herkul. Effect of physical disturbance and habitat-modifying species on sediment properties and benthic communities in the northern Baltic Sea. *Phd thesis*, page 48, 2010.

J. T. Holt and I. D. James. An s coordinate density evolving model of the northwest European continental shelf: 1 model description and density structure. *J. Geophys. Res. C*, 106:14015–14034, 2001a.

J. T. Holt and I. D. James. An s coordinate density evolving model of the northwest European continental shelf: 1 model description and density structure. *J. Geophys. Res. C*, 106:14035–14053, 2001b.

M. J. Howarth, R. Proctor, P. J. Knight, M. J. Smithson, and D. K. Mills. The Liverpool Bay Coastal Observatory towards the goals. *Proc Oceans 06, 18-21 September 2006, Boston, IEEE.*, page 6, 2006.

P. A. E. M. Janssen. Progress in ocean wave forecasting. *J. Comp. Phys.*, 227:3572–3594, 2008.

J.E. Jones. Coastal and shelf-sea modelling in the European context. *Oceanography and Marine Biology: an Annual Review*, 40:37–141, 2002.

J. M. J. Journèe and W.W. Massie. *Offshore hydrodynamics*, volume 4. Delft University of Technology, 2001.

G. J. Komen, L. Cavaleri, M. Donelan, K. Hasselmann, S. Hasselman, and P.A.E.M. Janssen. *Dynamics and Modelling of Ocean Waves.* Cambridge University Press, 1994.

J. Leake, J. Wolf, J. Lowe, P. Stansby, G. Jacoub, R. Nicholls, M. Mokrech, S. Nicholson-Cole, M. Walkden, and A. Watkinson. Predicted wave climate for the UK: towards an integrated model of coastal impacts of climate change. In *Proceeding of the Tenth International Conference on Estuarine and Coastal Modeling Congress*, pages 393–406, 2007.

L. A. Levin. Influence of sediment transport on short-term recolonization by seamount infauna. *Mar. Ecol. Prog. Ser.*, 123:163–175, 1995.

O. S. Madsen. Spectral wave-current bottom boundary layer flows. in: Coastal engineering 1994: Proceedings, 24th international conference, coastal engineering research council. *American Society of Civil Engineers, Kobe, Japan*, pages 384–398, 1994.

D. Maréchal. *A soil-based approach to rainfall-runoff modelling in ungauged catchments for England and Wales.* PhD thesis, Cranfield University, 2004.

D. Maurer, R. T. Keck, J. C. Tinsman, and W. A. Leathem. Vertical migration and mortality of benthos in dredged material: Part i mollusca. *Mar. Env. Res.*, 4:299–319, 1981a.

D. Maurer, R. T. Keck, J. C. Tinsman, and W. A. Leathem. Vertical migration and mortality of benthos in dredged material: Part i crustacea. *Mar. Env. Res.*, 5:301–317, 1981b.

J. Monbaliu, R. Padilla-Hernndeza, J. C. Hargreaves, J. C. Carretero Albiach, W. Luo, M. Sclavo, and H. Gunther. The spectral wave model, WAM, adapted for applications with high spatial resolution. *Coastal Eng.*, 41:41–62, 2000.

D. Myrhaug and L. E. Holmedal. Mobile layer thickness in sheet flow beneath random waves. *Coastal Engineering*, 54(8):577 – 585, 2007.

S. P. Neill, J. D. Scourse, and K. Uehara. Evolution of bed shear stress distribution over the northwest European shelf seas during the last 12,000 years. *Ocean Dynamics*, 60:1139–1156, 2010.

S. Pan, B. OConnor, C Vincent, D. Reeve, J. Wolf, M. Davidson, A. Dolphin, P. Thorne, P. Bell, A. Souza, T. Chesher, H. Johnson, and A. Leadbetter. Larger-scale morphodynamic impacts of segmented shore-parallel breakwaters on coasts and beaches: An overview of the LEACOAST2 project. *Shore & Beach (Journal of ASBPA)*, 78 (4/1), 2010.

A. Sana and H. Tanaka. Full-range equation for wave boundary layer thickness. *Coastal Engineering*, 54(8):639 – 642, 2007.

M. Schratzberger, H.L. Rees, and S.E Boyd. Effects of the simulated deposition of dredged material on the structure of nematode assemblages the role of burial. *Marine Biology.*, 136:519–530, 2000.

R. L. Soulsby. Bed shear-stresses due to combined waves and currents, in advances in coastal morphology. Technical report, Delft Hydraulics, Delft, the Netherlands, 1995.

A. Sterl and S. Caires. Climatology, variability and extrema of ocean waves: the web-based knmi/era-40 wave atlas. *International Journal of Climatology*, 25(7):963–977, 2005.

S.M. Uppala, P.W. Kalberg, A.J. Simmons, U. Andrae, V. da Costa Bechtold, M. Fiorino, J. K. Gibson, J. Haseler, A. Hernandez, G. A. Kelly, X. Li, K. Onogi, S. Saarinen, N. Sokka, R.P. Allan, E. Anderson, K. Arpe, M.A. Balmaseda, A.C.M Beljaars, L. van den Berg, J. Bidlot, N. Borman, S. Caires, A. Dethof, M. Dragosavac, M. Fisher, M. Fuentes, S. Hagemann, E. Holm., B. J. Hoskins, L. Isaksen, P.A.E.M Janssen, R. Jenne, A. P. McNally, J. F. Mahfouf, j. J Mocrette, N.A. Rayner, R.W. Saunders, P. Simon, A. Sterl, K.E. Trenberth, A. Untch, D. Vasiljevic, P. Viterbo, and J. Woollen. The ERA-40 re-analysis. *Quarterly J. of the Royal Met. S.*, 131: 2961–3012, 2005.

R. M. Warwick and R.J. Uncles. The distribution of benthic macrofauna associations in the Bristol Channel in relation to tidal stress. *Mar. Ecol. Prog. Ser.*, 3:97–103, 1980.

W. Weibull. A statistical distribution function of wide applicability. *J. Appl. Mechanics*, 18:293–297, 1951.

P. L. Wiberg and C. R. Sherwood. Calculating wave-generated bottom orbital velocities from surface-wave parameters. *Computers and Geosciences*, 34:1243–1262, 2008.

J. Williams and K. J. Horsburgh. Operational storm surge forecasting with 3.5km NISE10 model. *POL Internal Document*, 199:19, 2010.

J Wolf. The analysis of bottom pressure and current data for waves. In *Seventh International Conference on Electronic Engineering in Oceanography, 1997. Technology Transfer from Research to Industry.*, 1997.

J. Wolf. Coupled wave and surge modeling and implications for coastal flooding. *Advances in Geosciences.*, 17:19–22, 2008.

J. Wolf, A. J Souza, P. S. Bell, P. D. Thorne, R. D. Cooke, and S. Pan. Wave, currents and sediment transport observed during the LEACOAST2 experiment. In *PECS 2008: Physics of Estuaries and Coastal Seas, Liverpool, UK, 25th - 29th August 2008. Liverpool*, pages 373–376. PECS, 2008.

J. Wolf, P. Thorne, P. Bell, R. Cooke, and A. Souza. Waves, currents and sediment transport observed during the LEACOAST2 experiment. paper A.4 in modelling the effect of nearshore detached breakwaters on sandy macro-tidal coasts. Technical report, Environment Agency Report, 2010.

J. Wolf, J. Brown, and M. J. Howarth. The wave climate of Liverpool Bay - observations and modelling. *Ocean Dynamics*, 61:639–655, 2011.

D. K. Woolf, P. G. Challenor, and P. D. Cotton. The variability and predictability of North Atlantic wave climate. *J. Geophys. Res. C*, 10:1–14, 2002.

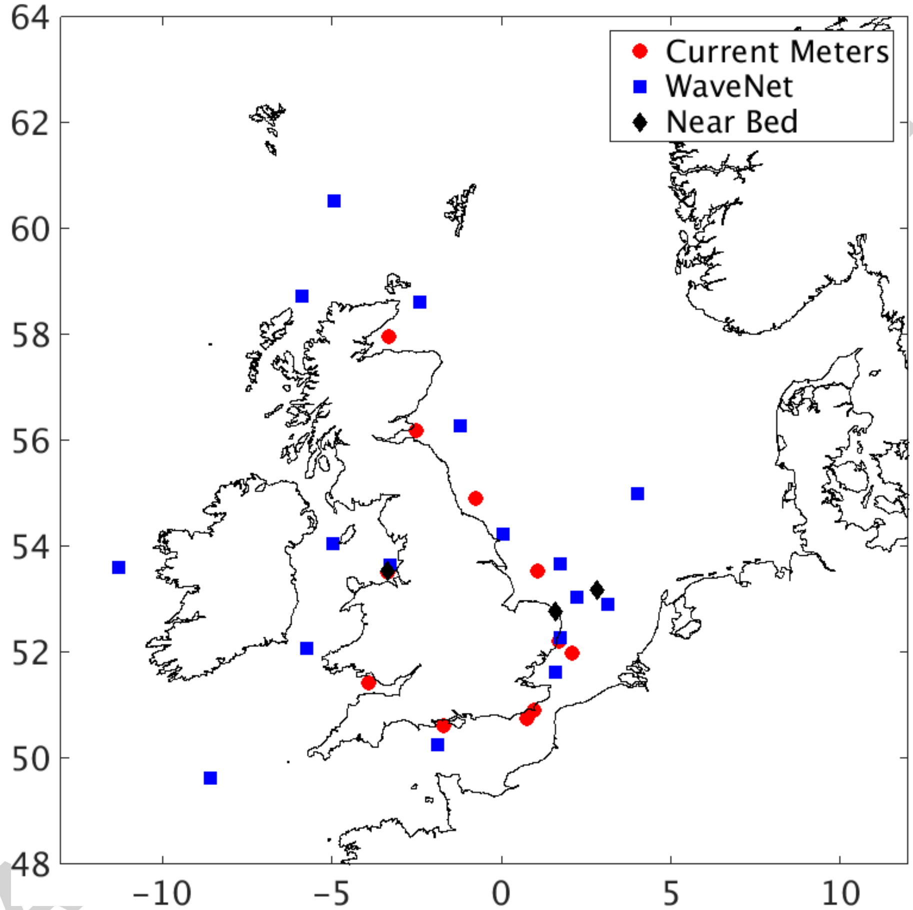

Figure 1: Model domain and locations of observations. WaveNet locations are marked with a blue squares, the current meters are represented by a red circles, and the bottom lander data are located at the black diamonds. N.B. In Liverpool bay the WaveNet and bottom lander sites are very closely located.

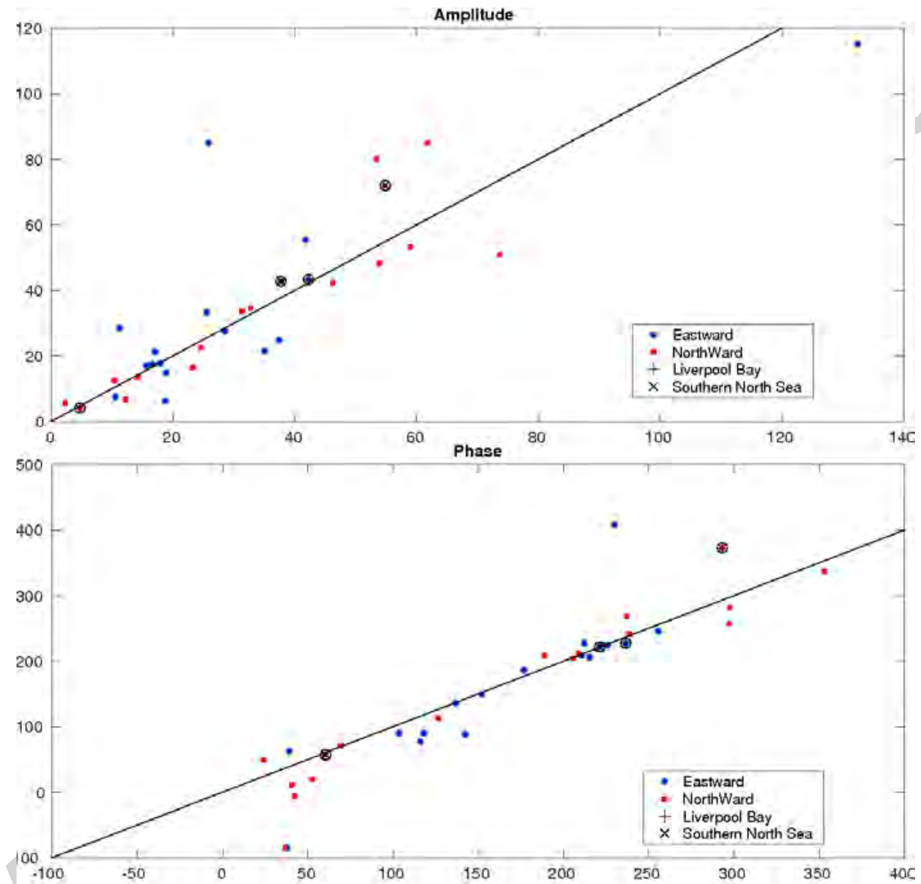

Figure 2: Scatter plots of amplitude (top) and phase (below) for M2 tidal currents observed around the Continental Shelf. The eastward currents are maked by blue circles, and the northward currents by red squares. Sites close to bottom lander locations are also highlighted

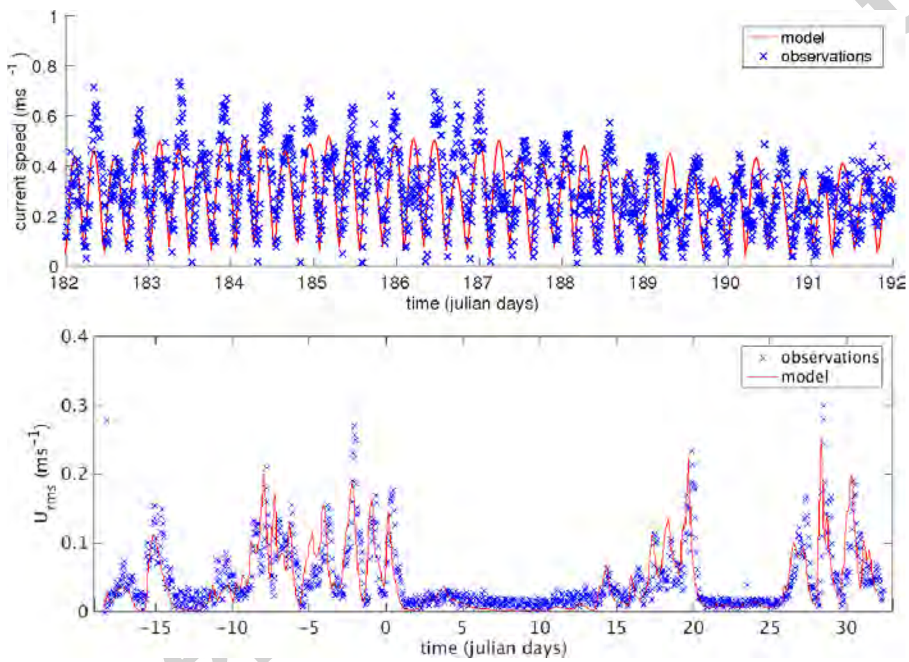

Figure 3: Time series of burst-averaged bottom current speed (top) during July 2007, and wave bottom orbital velocity (below) covering part of December 2007 and January 2008 (time is is Julian days). The observations are recorded at a site in Liverpool Bay (53°32.07N, 03°21.35W, and the closest model point is selected for comparison.

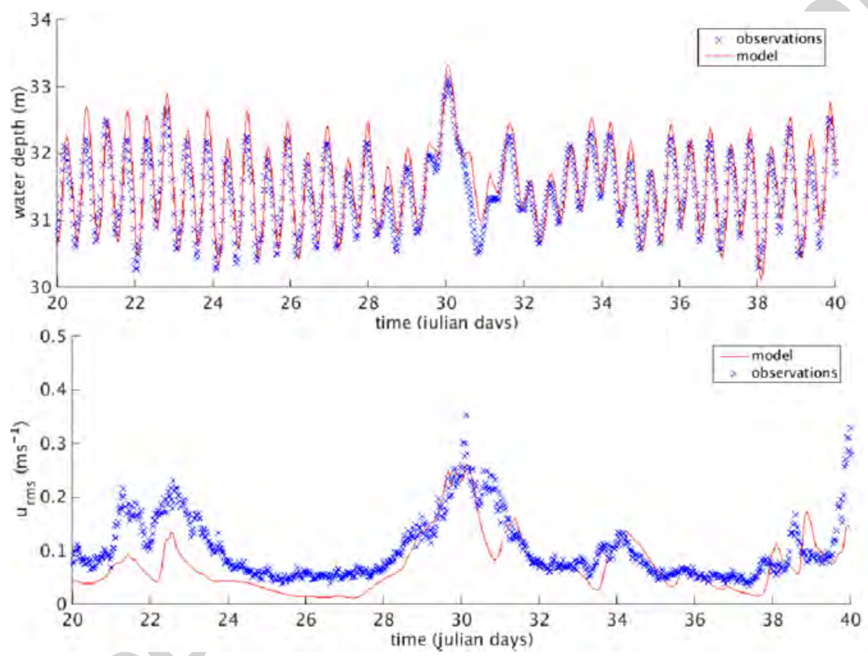

Figure 4: A comparison of water level (top) and wave bottom orbital velocity (below) at the Southern North Sea site during January 2000. The observed data is shown in blue crosses, and the modelled data as solid red lines.

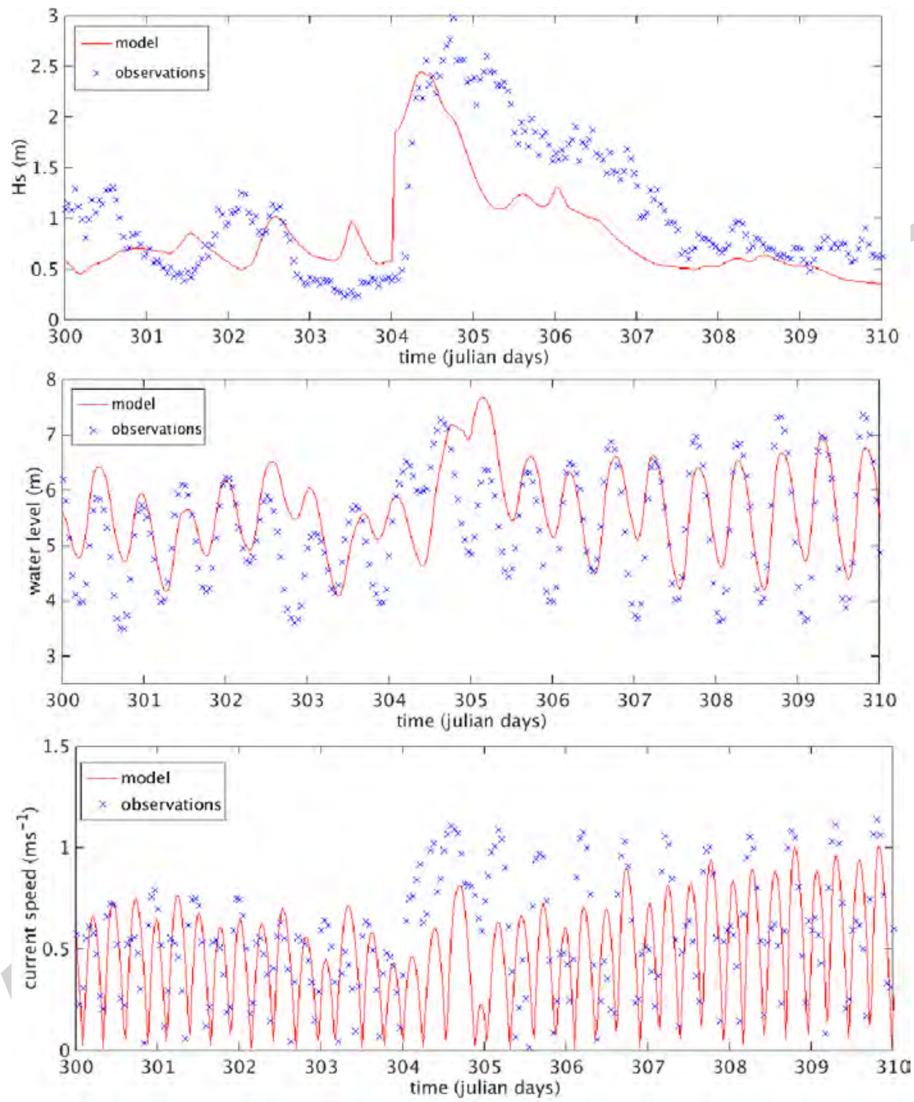

Figure 5: Time series of significant wave height (top), water level (centre), and burst-averaged bottom current speed (below) recorded at a site at Sea Palling (52°47.16N, 01°36.2E,) covering part of October and November 2006 (time is is Julian days)

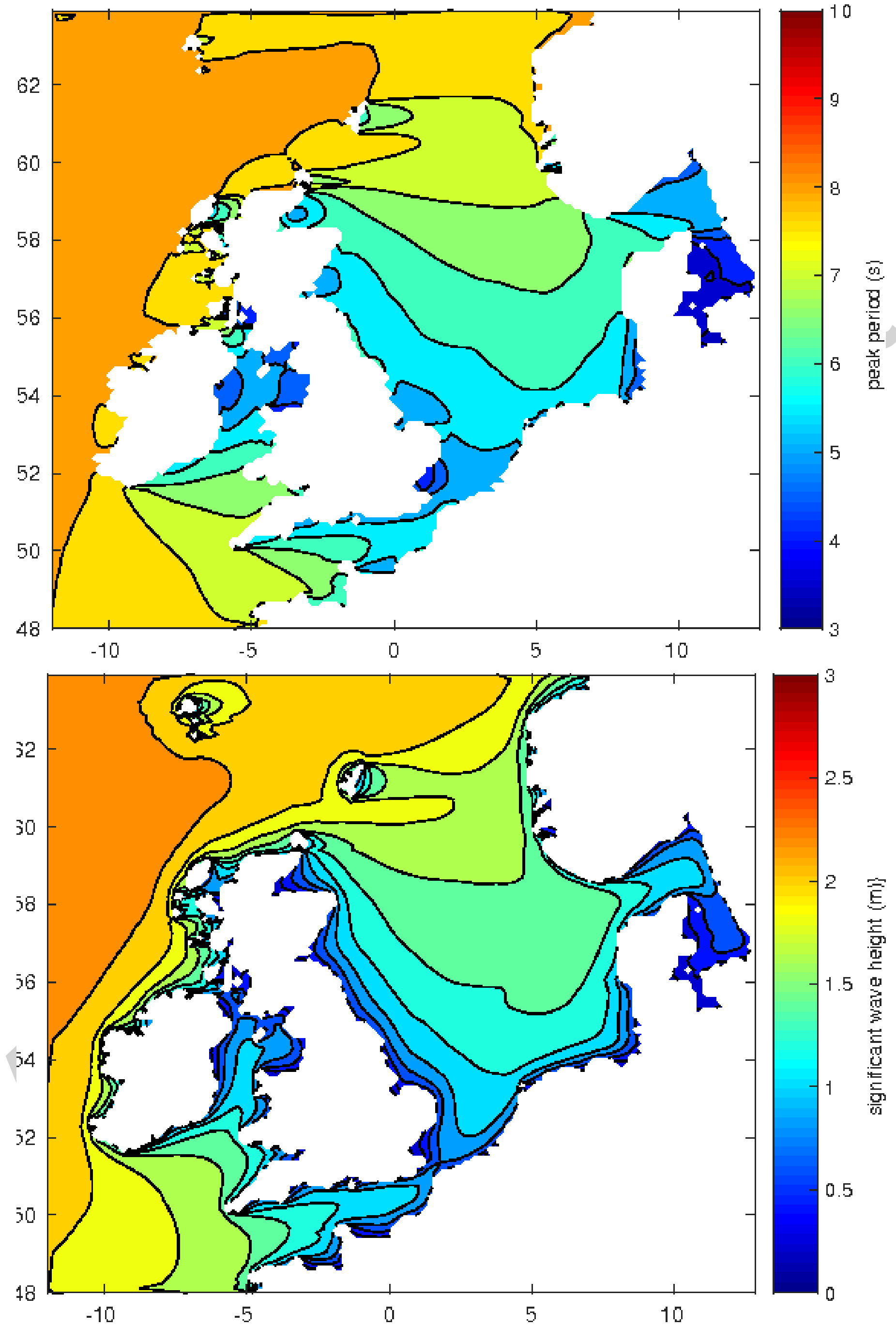

Figure 6: Top: Distribution of mean WAM modelled wave heights (m), and (below) average of the period of the spectral peak (s) from 10 years of data (1999-2008).

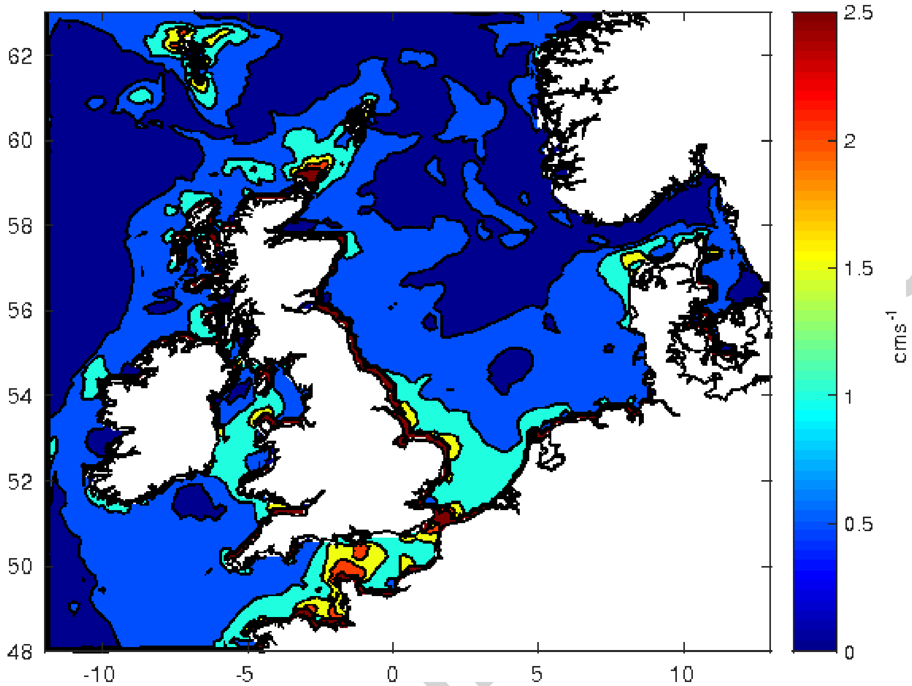

Figure 7: Distribution of maximum POLCOMS modelled currents for a typical year (2006).

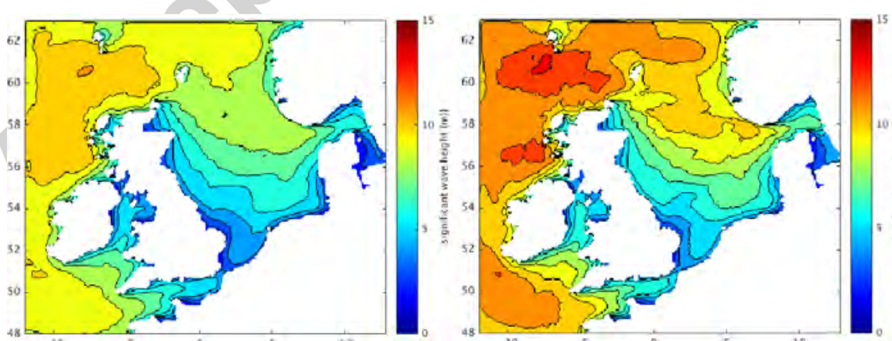

Figure 8: Distribution of extreme significant wave height (WAM modelled using years 1999-2008) for a 1 year return period (left) and a 50y year return period (right).

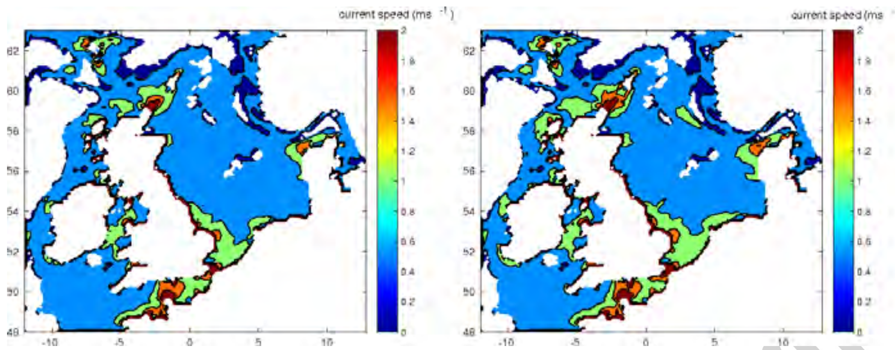

Figure 9: Contour maps showing the predictions of maximum current speeds (ms^{-1}) experienced across the UK continental shelf for a 1 year return period (left) and 50 year return period (right).

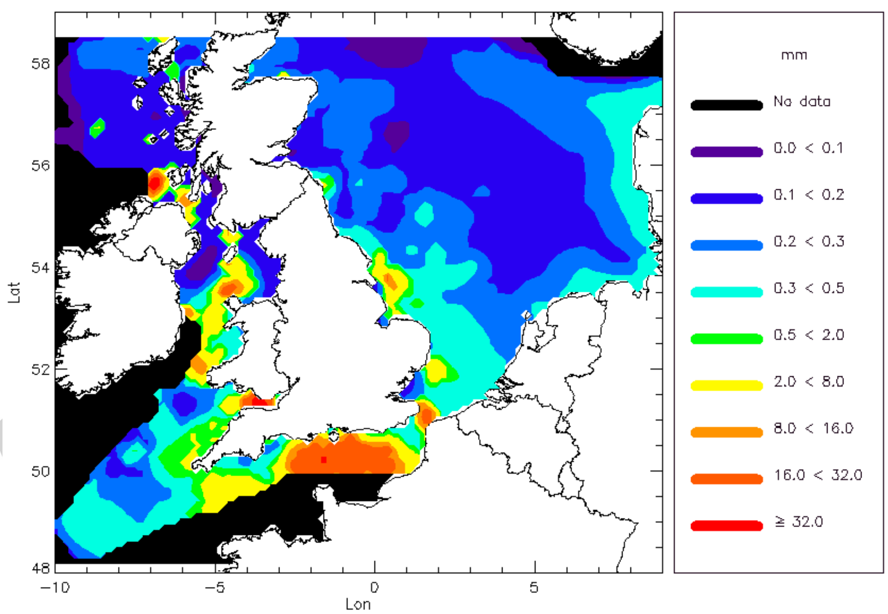

Figure 10: Contour maps showing distribution of median grain sizes used to calculate bottom roughness for non rippled beds. Note, the regions shown include mud, sand and gravel substrates as well as regions of mixed sediments.

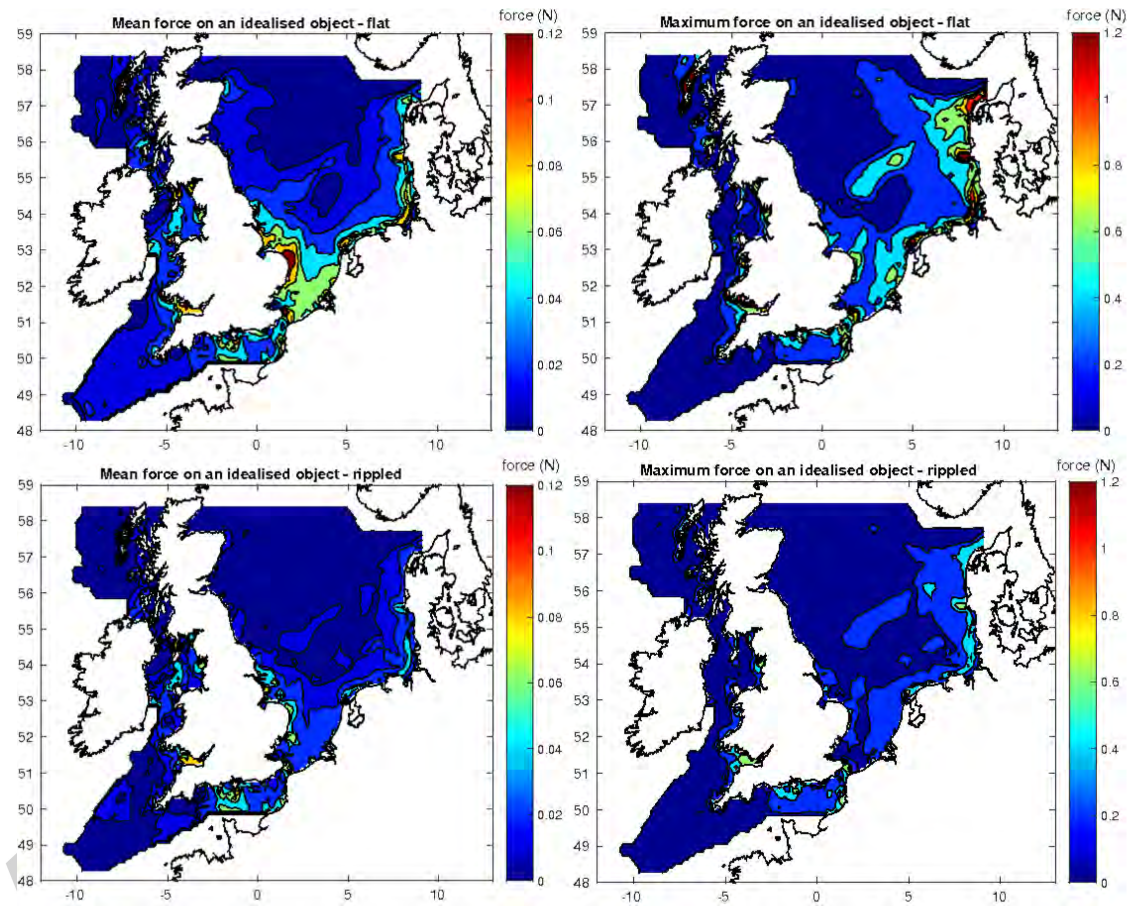

Figure 11: Contour maps showing the mean (left) and maximum (right) combined benthic force (N) experienced by an idealised object. For a flat bed (top) and rippled bed (below).